NONLINEAR DYNAMICS OF AN SMA LARGE-SCALE SPACE STRUCTURE

Aline S. de Paula, alinedepaula@unb.br
Universidade de Brasília
Department of Mechanical Engineering
70.910.900 – Brasília – DF – Brazil

Marcelo A. Savi, savi@mecanica.ufrj.br
Universidade Federal do Rio de Janeiro
COPPE – Department of Mechanical Engineering
21.941.972 – Rio de Janeiro – RJ, Brazil, P.O. Box 68.503

Dimitris C. Lagoudas, lagoudas@tamu.edu
Texas A&M University
Department of Aerospace Engineering
77843-3409 – College Station – Texas, USA

Abstract. *The dynamical analysis of large-scale structures is of special interest of aerospace applications, especially the ones involving smart materials. This paper deals with an archetypal system with two degrees of freedom resembled to the use of SMA elements as vibration isolation systems on a sparse aperture satellite array. The system has SMA elements in two perpendicular directions connected to a mass. Each SMA element is connected to a base structure. Numerical tests of this system are of concern showing the general dynamical behavior of the system.*

Keywords*: Shape memory alloys, smart structures, aerospace structures, nonlinear dynamics.*

1. INTRODUCTION

The dynamical response of shape memory alloy (SMA) systems presents a very rich and complex behavior due to the remarkable thermomechanical characteristics of SMAs. Periodic, quasi-periodic and chaotic responses are usually presented for dynamical system with SMA elements. There are several researches efforts dealing with this kind of systems. Savi and Braga (1993a) treated the dynamical response of SMA systems showing periodic and chaotic behaviors. Machado *et al.* (2004) discussed bifurcation and crises in an SMA oscillator. Both articles employed a polynomial constitutive model to describe the thermomechanical behavior of SMAs. Savi and Braga (1993b) studied an SMA oscillator employing another constitutive model to describe the restitution force of the oscillator. Lacarbonara *et al.* (2004) investigated the nonlinear response of a 1DOF SMA oscillator with a thermomechanical constitutive model and numerically demonstrated that a rich class of solutions, including discontinuity of frequency responses, quasi-periodicity and chaos could arise in nearly adiabatic conditions. Bernardini & Rega (2005) investigated a 1DOF system by considering a different thermomechanical model presenting the same richness for SMA oscillators. Aspects as nonlinear resonant conditions and thermomechanical coupling influence were treated. Savi *et al.* (2008) discussed the SMA response by considering a constitutive model that matches experimental data for quasi-static analysis. Investigations included tension-compression asymmetry and showed interesting results as multistability and chaos. Machado *et al.* (2009) proposed a procedure to evaluate Lyapunuv exponents in hysteretic systems, presenting SMA as an application of the general procedure. Once again, a rich response is related to the SMA system.

The dynamical behavior of SMA systems with multi-degrees of freedom seems to be much more complex. Savi & Pacheco (2002) presented an investigation considering one- and two-degree of freedom systems. Machado *et al.* (2003) revisited the 2DOF system showing different aspects of bifurcation of chaos. Large-scale structures might contain hundreds of connected nodes, being related to multi-degree of freedom systems. This kind of structure is of special interest for aerospace applications including antennas. Therefore, aerospace industry demands for a general comprehension of dynamical behavior of multi-degree of freedom SMA systems.

A typical large-scale structure with embedded SMA actuators is shown in Figure 1, representing a two-dimensional lattice connected by SMA elements. An archetypal model of this large-scale structure is also represented in Figure 1, being composed by a single mass connected by SMA elements.

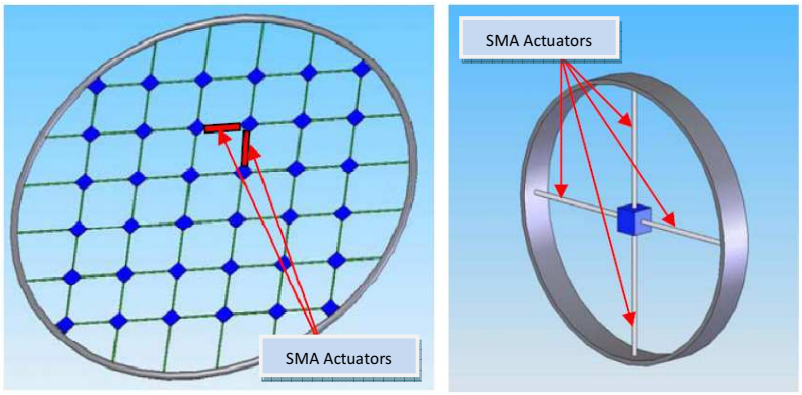

Figure 1 – SMA lattice.

Archetypal models are usually employed in stability analysis of structures, providing a global comprehension of the system behavior. The two-bar truss is an example of this kind of model that presents the snap-through behavior. This kind of systems allows one to analyze bifurcation scenarios related to stability changes associated with different characteristics of buckling behavior. Symmetric two-bar truss, known as the von Mises truss, represents one of the most popular system related to stability analysis. Savi *et al.* (2002a) analyzed a two-bar truss built with shape memory alloys (SMAs) that presents a very complex behavior. Recenttly, Savi & Nogueira (2010) revisited this truss using a more realistic constitutive model. The combination of geometrical and constitutive nonlinearities makes nonlinear dynamics of this structure especially complex.

This article deals with the dynamical response of a 2D SMA grid. Adaptive trusses with shape memory alloy actuators are examples of dynamical systems that may behave as the structure considered in this paper. An iterative numerical procedure based on the operator split technique (Ortiz *et al.*, 1983), the orthogonal projection algorithm (Savi *et al.*, 2002b) and the classical fourth order Runge-Kutta method is developed to deal with nonlinearities in the formulation. Numerical investigation is carried out considering free and forced responses of the pseudoelastic structure showing a number of interesting, complex behaviors.

2. MATHEMATICAL MODEL

The SMA lattice archetypal is composed of SMA elements in two perpendicular directions linked by a mass. Each SMA element is connected to a base structure, as shown in the schematic picture of Figure 2 that shows the SMA lattice at the ideal situation, where all SMA elements have the same length, L_0. The perturbed undeformed configuration represents a situation with perturbations from the ideal configuration in which all SMA elements are in a stress-free state. Figure 3 presents the perturbed undeformed configuration and the deformed configuration. This perturbed undeformed configuration may be related to a geometrical imperfection, for example. Figure 3 also presents the system of coordinates and the restitution forces acting in the mass.

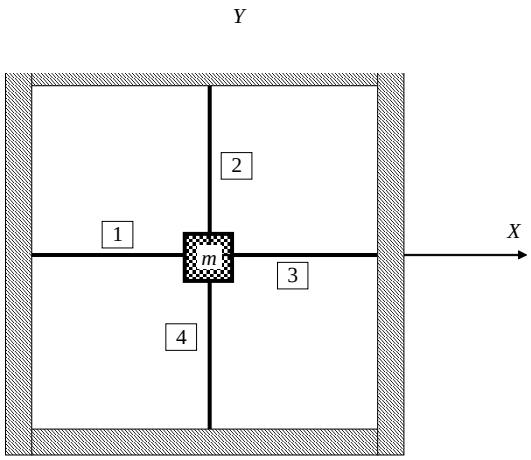

Figure 2 – Schematic picture of the SMA lattice.

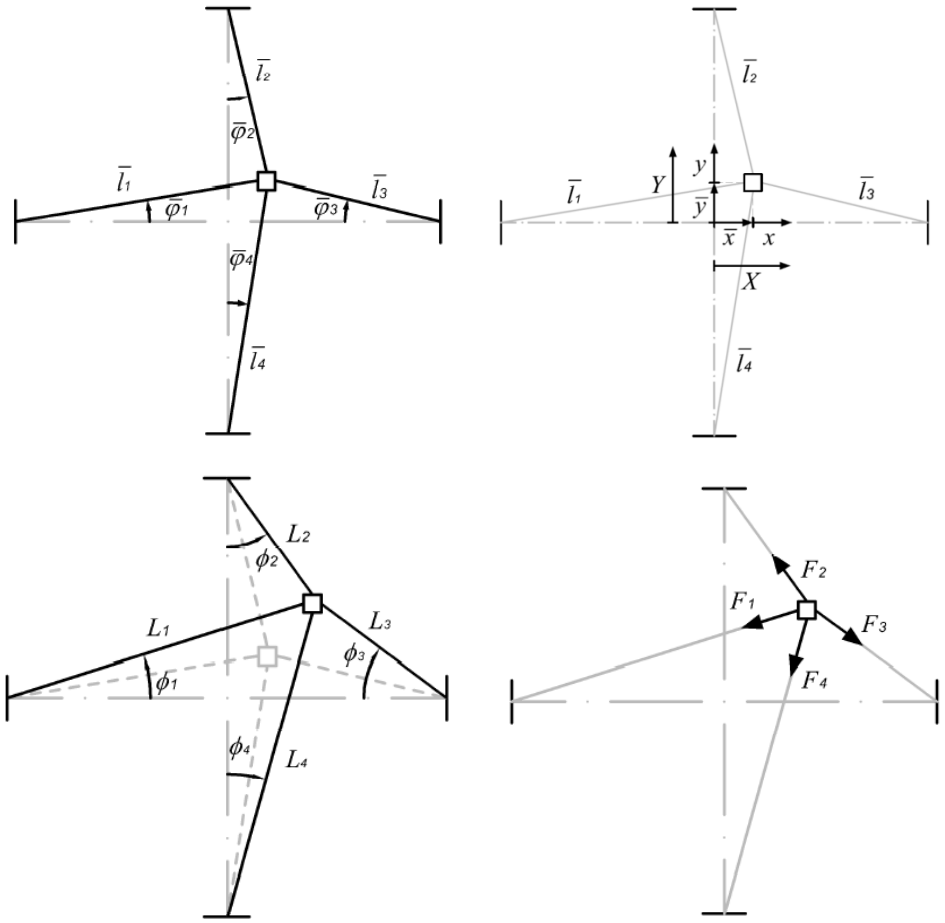

Figure 3 – Different configurations of the SMA lattice.

The SMA grid stress-free state is defined by bar-variables: $\bar{x}, \bar{y}, \bar{\varphi}_1, \bar{\varphi}_2, \bar{\varphi}_3, \bar{\varphi}_4$. This state defines the length of each SMA actuator, $\bar{l}_1, \bar{l}_2, \bar{l}_3, \bar{l}_4$, and the origin of the coordinate system (*x*, *y*). With the help of geometric considerations, it is possible to write:

$$\begin{aligned} X &= \bar{x} + x \\ Y &= \bar{y} + y \\ \phi_i &= \bar{\varphi}_i + \varphi_i \quad (i = 1,2,3,4) \end{aligned} \tag{1}$$

The length of each bar is given by:

$$\begin{aligned} L_1 &= \sqrt{(\bar{l}_1 \cos\bar{\varphi}_1 + x)^2 + (\bar{y} + y)^2}\ , \quad \bar{l}_1 = \sqrt{(\bar{l}_1 \cos\bar{\varphi}_1)^2 + \bar{y}^2} \\ L_2 &= \sqrt{(\bar{l}_2 \cos\bar{\varphi}_2 - y)^2 + (\bar{x} + x)^2}\ , \quad \bar{l}_2 = \sqrt{(\bar{l}_2 \cos\bar{\varphi}_2)^2 + \bar{x}^2} \\ L_3 &= \sqrt{(\bar{l}_3 \cos\bar{\varphi}_3 - x)^2 + (\bar{y} + y)^2}\ , \quad \bar{l}_3 = \sqrt{(\bar{l}_3 \cos\bar{\varphi}_3)^2 + \bar{y}^2} \\ L_4 &= \sqrt{(\bar{l}_4 \cos\bar{\varphi}_4 + y)^2 + (\bar{x} + x)^2}\ , \quad \bar{l}_4 = \sqrt{(\bar{l}_4 \cos\bar{\varphi}_4)^2 + \bar{x}^2} \end{aligned} \tag{2}$$

These lengths can be used to evaluate the deformation of each bar as follows:

$$\varepsilon_i = \frac{L_i - \bar{l}_i}{\bar{l}_i} \quad (i = 1,2,3,4) \tag{3}$$

The angles that define the SMA actuator position are:

$$\cos\phi_1 = \frac{\bar{l}_1\cos\bar{\varphi}_1 + x}{L_1}\ , \quad \sin\phi_1 = \frac{\bar{y} + y}{L_1}$$
$$\cos\phi_2 = \frac{\bar{l}_2\cos\bar{\varphi}_2 - y}{L_2}\ , \quad \sin\phi_2 = \frac{\bar{x} + x}{L_2} \tag{4}$$
$$\cos\phi_3 = \frac{\bar{l}_3\cos\bar{\varphi}_3 - x}{L_3}\ , \quad \sin\phi_3 = \frac{\bar{y} + y}{L_3}$$
$$\cos\phi_4 = \frac{\bar{l}_4\cos\bar{\varphi}_4 + y}{L_4}\ , \quad \sin\phi_4 = \frac{\bar{x} + x}{L_4}$$

By assuming a mass *m* excited by an external force characterized by a sinusoidal excitation with amplitude F_x and F_y in direction *x* and *y*, respectively, and frequency ω_x and ω_y in the same directions. Besides, it is assumed that all dissipations different from hysteretic behavior is due to a viscous damping, described by the coefficient *c*. The balance of momentum is expressed through the following equations of motion:

$$m\ddot{x} + c\dot{x} + F_1\cos\phi_1 - F_2\sin\phi_2 + F_3\cos\phi_3 + F_4\sin\phi_4 = F_x\sin(\omega_x t) \tag{5}$$

$$m\ddot{y} + c\dot{y} + F_1\sin\phi_1 + F_2\cos\phi_2 - F_3\sin\phi_3 + F_4\cos\phi_4 = -mg + F_y\sin(\omega_y t) \tag{6}$$

where F_i (i = 1,2,3,4) is the force on actuator *i*. The thermomechanical description of this force may be done by a proper constitutive model described in the next subsection.

2.1. Constitutive Model

The description of each SMA actuator force F_i is related to the SMA thermomechanical behavior and it is assumed that phase transformations are homogeneous through the element. There are different ways to describe the SMA behavior and here, a constitutive model with internal variables previously discussed in different references (Savi *et al.*, 2002b, Baêta-Neves *et al.*, 2004, Paiva *et al.*, 2005, Savi & Paiva, 2005; Monteiro *et al.*, 2009; Aguiar *et al.*, 2010; Oliveira *et al.*, 2010) is employed.

In order to present the constitutive equations, let us consider strain (ε), temperature (T), and three more state variables associated with the volume fraction of each phase: β^{M+} is associated with tensile detwinned martensite, β^{M-} is related to compressive detwinned martensite, β^{A} represents austenite. Actually, it is considered a fourth phase βM related to twinned martensite, that can be obtained from phase coexistence condition ($\beta^{M} = 1 - \beta^{M+} + \beta^{M-} + \beta^{A}$). With this assumption, it is possible to obtain a complete set of constitutive equations that describes the thermomechanical behavior of SMAs as follows:

$$\sigma = E\varepsilon + [\alpha + E\alpha^h](\beta^{M-} - \beta^{M+}) - \Omega(T - T_0) \tag{7}$$

$$\dot{\beta}^{M+} = \frac{1}{\eta^{M+}}\left\{ \alpha\varepsilon + \Lambda^M + [2\alpha^h\alpha + E(\alpha^h)^2](\beta^{M-} - \beta^{M+}) + \alpha^h\left[E\,\varepsilon - \Omega(T - T_0)\right] - \partial_1 J_\pi \right\} + \partial_1 J_\chi \tag{8}$$

$$\dot{\beta}^{M-} = \frac{1}{\eta^{M-}}\left\{ -\alpha\varepsilon + \Lambda^M - [2\alpha^h\alpha + E(\alpha^h)^2](\beta^{M-} - \beta^{M+}) - \alpha^h\left[E\,\varepsilon - \Omega(T - T_0)\right] - \partial_2 J_\pi \right\} + \partial_2 J_\chi \tag{9}$$

$$\dot{\beta}^{A} = \frac{1}{\eta^{A}}\left\{ -\frac{1}{2}\left(E^A - E^M\right)\left[\varepsilon + \alpha^h(\beta^{M-} - \beta^{M+})\right]^2 + \Lambda^A + \right.$$
$$\left. + \left(\Omega^A - \Omega^M\right)(T - T_0)\left[\varepsilon + \alpha^h(\beta^{M-} - \beta^{M+})\right] - \partial_3 J_\pi \right\} + \partial_3 J_\chi \tag{10}$$

where $E = E^M + \beta^A\left(E^A - E^M\right)$ is the elastic modulus while $\Omega = \Omega^M + \beta^A\left(\Omega^A - \Omega^M\right)$ is related to the thermal expansion coefficient. Note that subscript "*A*" refers to austenitic phase, while "*M*" refers to martensite. Moreover, parameters $\Lambda^M = \Lambda^M(T)$ and $\Lambda^A = \Lambda^A(T)$ are associated with phase transformations stress levels. Parameter α^h is

introduced in order to define the horizontal width of the stress-strain hysteresis loop, while α helps vertical hysteresis loop control on stress-strain diagrams.

The terms $\partial_n J_\pi$ (n = 1,2,3) are sub-differentials of the indicator function J_π with respect to β_n (Rockafellar, 1970). The indicator function $J_\pi = J_\pi(\beta_1, \beta_2, \beta_3)$ is related to a convex set π, which provides the internal constraints related to the phases' coexistence. With respect to evolution equations of volume fractions, η represent the internal dissipation related to phase transformations. Moreover $\partial_n J_\chi$ (n = 1,2,3) are sub-differentials of the indicator function J_χ with respect to $\dot{\beta}^n$ (n = 1,2,3) (Rockafellar, 1970). This indicator function is associated with the convex set χ, which establishes conditions for the correct description of internal subloops due to incomplete phase transformations and also avoids phase transformations $M^+ \rightarrow M$ or $M^- \rightarrow M$.

Concerning the parameters definition, temperature dependent relations are adopted for Λ_M and Λ_A as follows:

$$\Lambda^M = \begin{cases} -\Lambda_0^M + \dfrac{\Lambda_1^M}{T_M}(T - T_M) & \text{if} \quad T > T_M \\ -\Lambda_0^M & \text{if} \quad T \le T_M \end{cases} \tag{11}$$

$$\Lambda^A = \begin{cases} -\Lambda_0^A + \dfrac{\Lambda_1^A}{T_M}(T - T_M) & \text{if} \quad T > T_M \\ -\Lambda_0^A & \text{if} \quad T \le T_M \end{cases} \tag{12}$$

Here, T_M is the temperature below which the martensitic phase becomes stable in a stress-free state. Besides, Λ_0^M, Λ_1^M, Λ_0^A and Λ_1^A are parameters related to critical stress for phase transformation.

In order to contemplate different characteristics of the kinetics of phase transformation for loading and unloading processes, it is possible to consider different values to the internal dissipation parameter η_n ($n = M^+, M^-, A$): η_n^L and η_n^U during loading and unloading process, respectively. For more details about the constitutive model, see Paiva *et al.* (2005) and Savi & Paiva (2005).

2.2. Equations of Motion

Based on constitutive modeling, it is possible to calculate the force in each SMA actuator and the equations of motion are given by:

$$m\ddot{X} + c\dot{X} + F_1\cos\phi_1 - F_2\sin\phi_2 + F_3\cos\phi_3 + F_4\sin\phi_4 = F_x\sin(\Omega_x t) \tag{13}$$

$$m\ddot{Y} + c\dot{Y} + F_1\sin\phi_1 + F_2\cos\phi_2 - F_3\sin\phi_3 + F_4\cos\phi_4 = -mg + F_y\sin(\Omega_y t) \tag{14}$$

$$F_i = \frac{E_i A_i}{L_i}\varepsilon_i + [\alpha_i + E_i\alpha_i^h](\beta_i^{M-} - \beta_i^{M+}) - \Omega_i(T_i - T_0), \quad (i = 1,2,3,4) \tag{15}$$

By defining the dimensionless variables:

$$\hat{x} = \frac{x}{L_0}; \quad \hat{y} = \frac{y}{L_0}; \quad \theta = \frac{T}{T_R}; \quad \tau = \omega_0 t \tag{16}$$

where L_0 is a reference length defined in the ideal configuration ($\bar{x} = \bar{y} = 0$; $\bar{\varphi}_1 = \bar{\varphi}_2 = \bar{\varphi}_3 = \bar{\varphi}_4 = 0$) as shown in Figure 2. Dimensionless equations of motion are given by:

$$\hat{x}'' + \xi\hat{x}' + \Gamma_1\cos\phi_1 - \Gamma_2\sin\phi_2 + \Gamma_3\cos\phi_3 + \Gamma_4\sin\phi_4 = \delta_x\sin(\varpi_x\tau) \tag{17}$$

$$\hat{y}'' + \xi\,\hat{y}' + \Gamma_1 \sin\phi_1 + \Gamma_2 \cos\phi_2 - \Gamma_3 \sin\phi_3 + \Gamma_4 \cos\phi_4 = -\frac{mg}{E_R A} + \delta_y \sin(\varpi_y \tau) \tag{18}$$

$$\Gamma_i = \mu_i^E \varepsilon_i + [\hat{\alpha}_i + \mu_i^E \hat{\alpha}_i^h](\beta_i^{M-} - \beta_i^{M+}) - \mu_i^\Omega (\theta_i - \theta_0) \quad (i = 1,2,3,4) \tag{19}$$

where

$$\omega_0^2 = \frac{E_R A}{mL_0};\ \ \xi = \frac{c}{m\omega_0}\ \ ;\ \ \hat{\alpha} = \frac{\alpha A}{mL_0\omega_0^2} = \frac{\alpha}{E_R};\ \ \hat{\alpha}^h = \frac{\alpha^h E_R A}{mL_0\omega_0^2} = \alpha^h;\ \delta = \frac{F_0}{mL_0\omega_0^2} = \frac{F_0}{E_R A};$$
$$\hat{\Omega} = \frac{\Omega_R A T_R}{mL_0\omega_0^2} = \frac{\Omega_R T_R}{E_R};\ \ \mu^E = \frac{E}{E_R};\ \ \mu^\Omega = \frac{\Omega}{\Omega_R};\ \ \varpi = \frac{\omega}{\omega_0} \tag{20}$$

From now on, $\hat{x}$ and $\hat{y}$ will be replaced by x and y, respectively.

3. NUMERICAL SIMULATIONS

Numerical simulations are performed employing the fourth-order Runge-Kutta scheme with time steps chosen to be less than $\Delta\tau = \pi/(400\varpi)$. In all simulations, we have used the material properties presented in Table 1, which represents typical SMA behavior obtained for a strain driving quasi-static simulation at T = 373K. It is considered that all SMA actuators have length, at ideal situation, of L_0=2.236m and a cross section area of A=0.25m^2. Therefore, the parameters defined in Equations (16) and (20) assume the values of $\omega_0^2 = 6\times10^9$, $\theta = 1.28$, $\hat{\alpha} = 2.78\times10^{-3}$, $\hat{\Omega} = 9.17\times10^{-4}$. Some simulations are performed considering two different situations: a perturbed undeformed configuration with an initial position of $\bar{x} = \bar{y} = 0.1$ and the ideal case where $\bar{x} = \bar{y} = 0$. Free and force vibrations are of concern. Concerning forced vibrations, only vertical excitation is treated, and therefore δ_x = 0. No other dissipation different from SMA hysteresis is considered and therefore, the viscous dissipation is neglected (ξ = 0). A pseudoelastic system is treated which means that the austenitic phase is stable at stress-free state.

Table 1. SMA constitutive parameters.

E_A (GPa)	E_M (GPa)	α (MPa)	α^h	Λ_0^M (MPa)	Λ_1^M (MPa)	Λ_0^A (MPa)	Λ_1^A (MPa)
54	54	150	0.052	0.15	41.5	0.63	185
Ω_A (MPa/K)	Ω_M (MPa/K)	T_M (K)	T_A (K)	η^L (MPa.s)	η^U (MPa.s)		
0.74	0.17	291.4	307.7	10	27		

3.1. Free Vibrations

Let us start with the free vibration analysis by considering an initial velocity in the x-direction and $\bar{x} = \bar{y} = 0.1$. Under this condition the system tends to dissipate energy due to the hysteresis loop. Results from simulations are presented in Figure 4 that presents two subspaces of the phase space related to the free-response of the structure. We called x-space, built with (x, x') and y-space (y, y'). Note that in the x-space, hysteretic behavior dissipates energy until elastic response is reached in the steady-state. The y-space presents response only at elastic regime. This behavior can be understood by observing the thermomechanical behavior of each SMA element. Figure 5 presents volume fraction evolution of each phase at each actuator while Figure 6 presents the stress-strain curves of each SMA actuator.

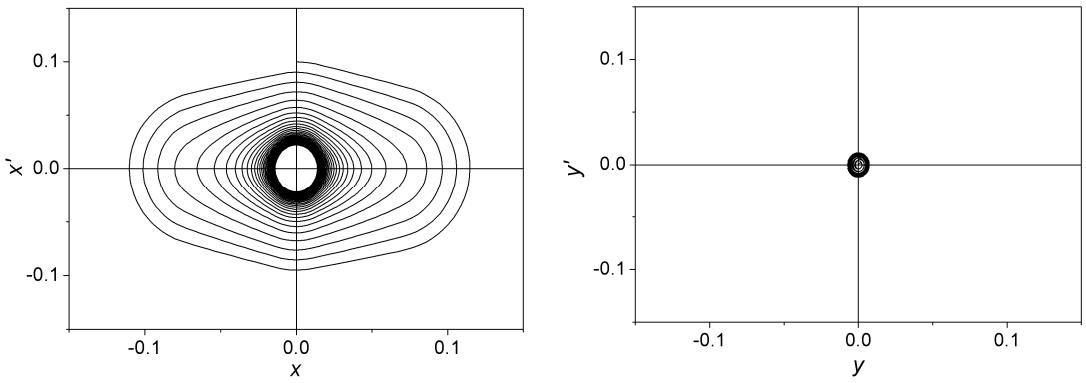

Figure 4. State space of the free response.

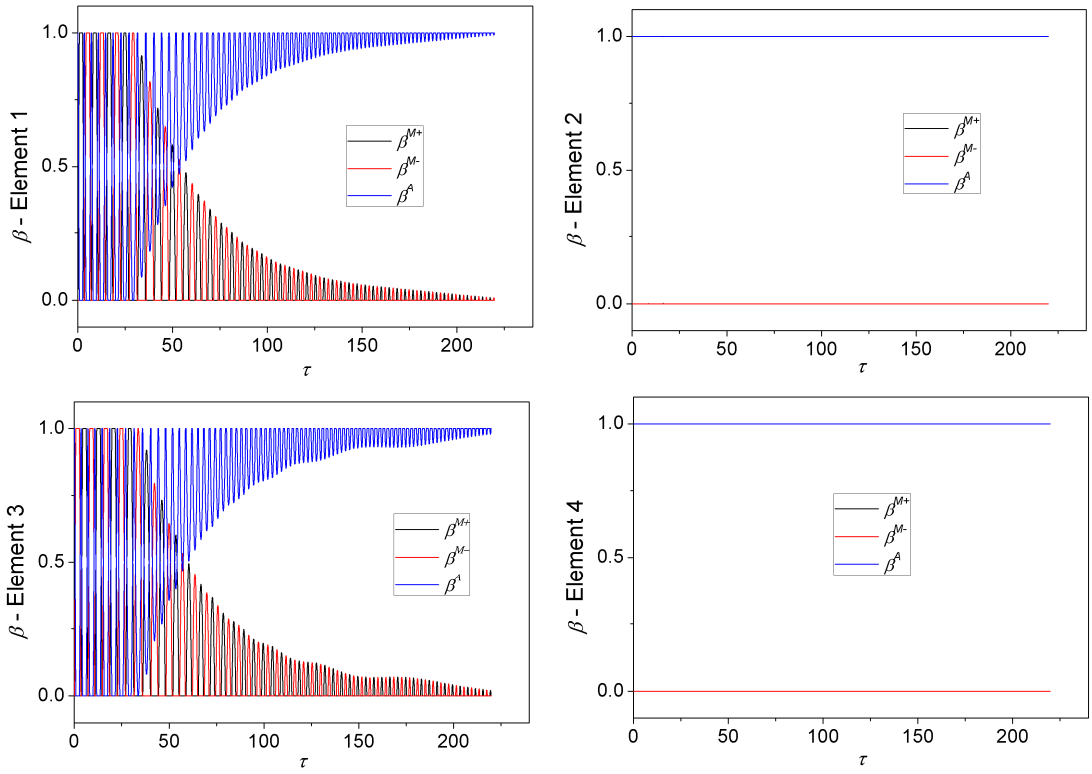

Figure 5. Volume fraction evolutions of the free response.

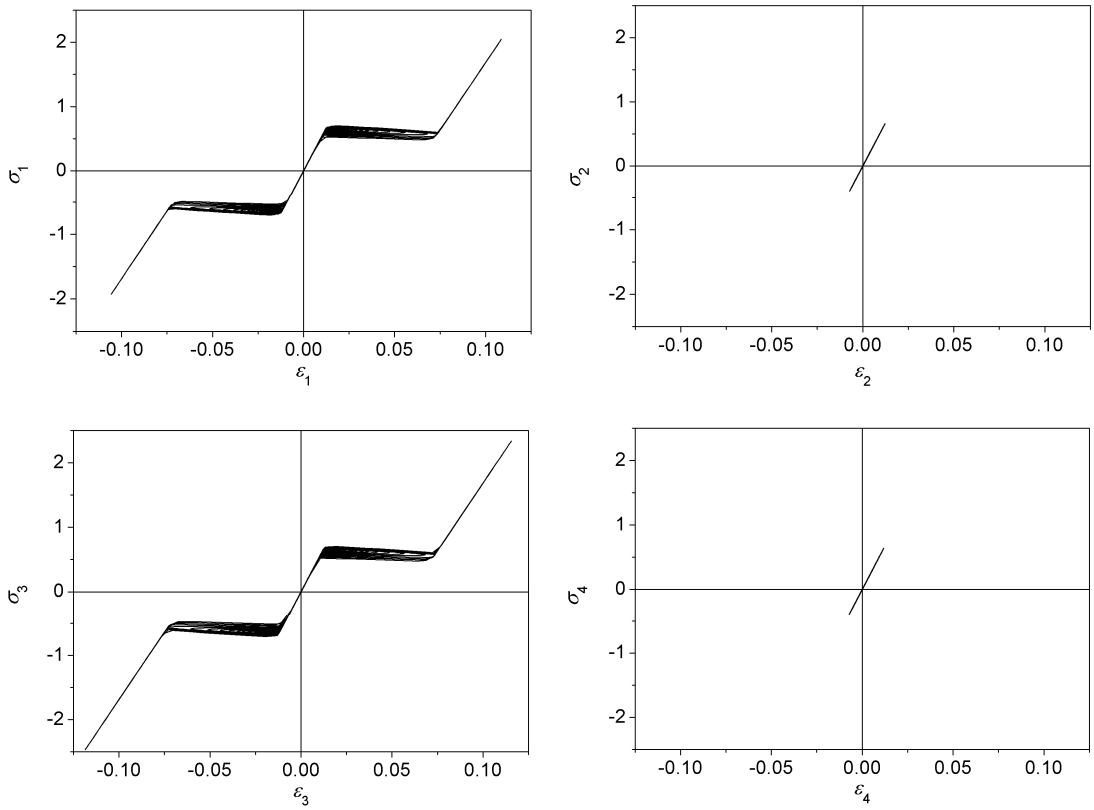

Figure 6. Stress-strain curves of the free response.

The coupling between both directions is caused by the perturbed undeformed configuration. By assuming that the undeformed configuration coincides with the ideal situation ($\bar{x} = \bar{y} = 0$), the system presents the same qualitative behavior except for the fact that the movement is restricted to the *x*-direction.

3.2. Forced Vibrations

This section considers the forced vibration analysis of the system. Initially, let us consider again the perturbed undeformed configuration with $\bar{x} = \bar{y} = 0.1$ and that $\delta_y = 0.04$ and $\Omega_y = 0.5$. Under this condition, the system presents a periodic response as shown in Figure 7. This steady-state response is related to phase transformations that preponderantly occur in vertical elements (2 and 4). Once again, the perturbed undeformed configuration promotes a coupling between *x*-*y* directions. Large transients are expected, especially in the *x*-direction due to a less amount of phase transformation.

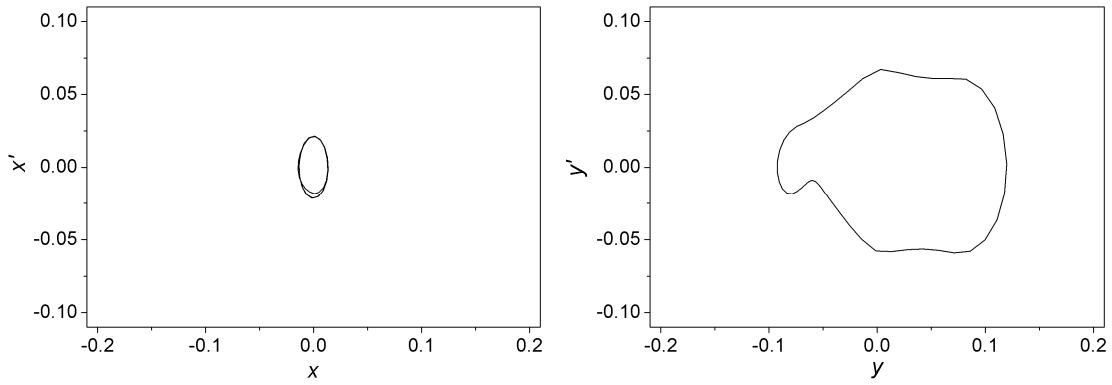

Figure 7. Periodic response due to an excitation $\delta_y = 0.04$ and $\Omega_y = 0.5$.

Let us now consider a different excitation, with greater amplitudes: $\delta_y = 0.4$ and $\Omega_y = 0.5$. This excitation produces a chaotic-like response as presented in Figure 8. The increase of the complexity of this response is due to the nonlinear response of all SMA elements. Basically, phase transformations are occurring in all the four actuators in contrast of the previous example, where only two actuators present large amount of phase transformations.

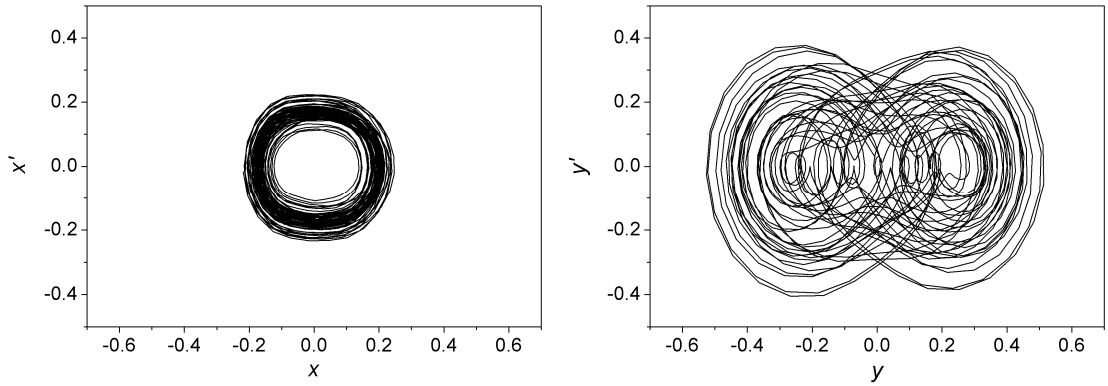

Figure 8. Chaotic-like response due to an excitation $\delta_y = 0.4$ and $\Omega_y = 0.5$.

By analyzing the ideal situation ($\bar{x} = \bar{y} = 0$) the coupling between *x*-*y* directions does not occur anymore. Therefore, the system dynamics is restricted to *y*-direction. Figure 9 presents excitation previously analyzed. By considering $\delta_y = 0.04$ and $\Omega_y = 0.5$, system presents a periodic response presented in the left panel of Figure 9. Note that this response has the same pattern of that obtained in Figure 7. By increasing the excitation parameters to $\delta_y = 0.4$ and $\Omega_y = 0.5$, the system response presents a periodic response (Figure 9, right panel) in contrast with the chaotic-like response of Figure 8.

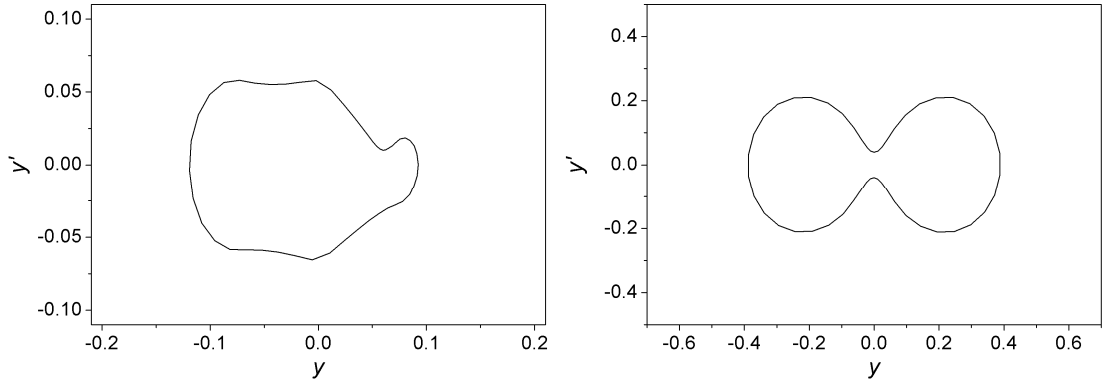

Figure 9. Forced vibration of the system when undeformed configuration coincides with ideal situation ($\bar{x} = \bar{y} = 0$). Left panel: $\delta_y = 0.04$ and $\Omega_y = 0.5$; Right panel: $\delta_y = 0.4$ and $\Omega_y = 0.5$.

4. CONCLUSIONS

This article deals with the dynamical response of a 2D-SMA grid that represents adaptive trusses with shape memory alloy actuators. An iterative numerical procedure based on the operator split technique, the orthogonal projection algorithm and the classical fourth order Runge-Kutta method is developed to deal with nonlinearities in the formulation. Numerical investigation is carried out considering free and forced responses of the pseudoelastic structure showing a number of interesting, complex behaviors. It is important to highlight how imperfections can alter system characteristics providing a coupling between both directions.

5. ACKNOWLEDGEMENTS

The authors would like to acknowledge the support of the Brazilian Research Agencies CNPq, CAPES and FAPERJ and through the INCT-EIE (National Institute of Science and Technology - Smart Structures in Engineering) the CNPq

and FAPEMIG. The Air Force Office of Scientific Research (AFOSR) is also acknowledged.

6. REFERENCES

Aguiar, R.A.A., Savi, M.A. & Pacheco, P.M.C.L., 2010, "Experimental and numerical investigations of shape memory alloy helical springs", Smart Materials and Structures, v.19, n.2, Article 025008, pp.1-9.

Baêta-Neves, A.P., Savi, M.A. & Pacheco, P.M.C.L., 2004, "On the Fremond's constitutive model for shape memory alloys", Mechanics Research Communications, 31 (6), pp.677-688.

Bazant, Z. P. & Cedolin, L., 1991, "Stability of structures", Oxford Press.

Bernardini, D. & Rega, G., 2005, "Thermomechanical modelling, nonlinear dynamics and chaos in shape memory oscillators", Mathematical and Computer Modelling of Dynamical Systems, v.11, n.3, pp.291-314.

Lacarbonara, W. & Vestroni, F, 2003, "Nonclassical responses of oscillators with hysteresis", Nonlinear Dynamics, v.32, pp.235-258.

Lacarbonara, W., Bernardini, D. & Vestroni, F., 2004, "Nonlinear thermomechanical oscillations of shape-memory devices", International Journal of Solids and Structures, v.41, n.5-6, pp.1209-1234.

Lagoudas, D.C. (2008), "Shape Memory Alloys: Modeling and Engineering Applications", Springer.

Machado, L.G. & Savi, M.A., 2003, "Medical applications of shape memory alloys", Brazilian Journal of Medical and Biological Research, v.36, n.6, pp.683-691.

Machado, L.G., Savi, M.A. & Pacheco, P.M.C.L., 2003, "Nonlinear dynamics and chaos in coupled shape memory oscillators", International Journal of Solids and Structures, v.40, n.19, pp.5139-5156.

Machado, L.G., Savi, M.A. & Pacheco, P.M.C.L., 2004, "Bifurcations and crises in a shape memory oscillator", Shock and Vibration, v.11, n.2, pp.67-80.

Machado, L.G., Lagoudas, D.C. & Savi, M.A., 2009, "Lyapunov exponents estimation for hysteretic systems", International Journal of Solids and Structures, v.46, n.6, pp.1269-1598.

Monteiro Jr, P.C.C., Savi, M.A., Netto, T.A. & Pacheco, P.M.C.L., 2009, "A phenomenological description of the thermomechanical coupling and the rate-dependent behavior of shape memory alloys", Journal of Intelligent Material Systems and Structures, v.20, n.14, pp.1675-1687.

Oliveira, S.A., Savi, M.A. & Kalamkarov, A.L., 2010, "A three-dimensional constitutive model for shape memory alloys", Archive of Applied Mechanics, v.80, n.10, pp.1163-1175.

Ortiz, M., Pinsky, P.M. & Taylor, R.L., 1983, "Operator split methods for the numerical solution of the elastoplastic dynamic problem", Computer Methods of Applied Mechanics and Engineering, 39, pp.137-157.

Paiva, A., Savi, M.A., Braga, A.M.B. & Pacheco, P.M.C.L., 2005, "A constitutive model for shape memory alloys considering tensile-compressive asymmetry and plasticity", International Journal of Solids and Structures, v.42, n.11-12, pp.3439-3457.

Paiva, A. & Savi, M.A., 2006, "An overview of constitutive models for shape memory alloys", Mathematical Problems in Engineering, v.2006, Article ID56876, pp.1-30.

Savi, M.A. & Braga, A.M. B., 1993a, "Chaotic vibrations of an oscillator with shape memory", Journal of the Brazilian Society of Mechanical Sciences and Engineering, v.XV, n.1, pp.1-20.

Savi, M.A. & Braga, A.M.B., 1993b, "Chaotic response of a shape memory oscillator with internal constraints", Proceedings of XII the Brazilian Congress of Mechanical Engineering (COBEM 93 - ABCM), Brasília, Brazil, pp.33-36.

Savi, M.A. & Nogueira, J.B., 2010, "Nonlinear Dynamics and Chaos in a Pseudoelastic Two-Bar Truss", Smart Materials & Structures, v.19, n.11, Article 1150222010, pp.1-11.

Savi, M.A. & Pacheco, P.M.L.C., 2002, "Chaos and hyperchaos in shape memory systems", International Journal of Bifurcation and Chaos, v.12, n.3, pp.645-657.

Savi, M.A., Pacheco, P.M.C.L. & Braga, A.M.B., 2002a, "Chaos in a shape memory two-bar truss", International Journal of Non-linear Mechanics, v.37, n.8, pp.1387-1395.

Savi, M.A., Paiva, A., Baêta-Neves, A.P. & Pacheco, P.M.C.L., 2002b, "Phenomenological modeling and numerical simulation of shape memory alloys: A thermo-plastic-phase transformation coupled model", Journal of Intelligent Material Systems and Structures, v.13, n.5, pp.261-273.

Savi, M.A. & Paiva, A., 2005, "Describing internal subloops due to incomplete phase transformations in shape memory alloys", Archive of Applied Mechanics, v.74, n.9, pp.637-647.

Savi, M.A., Sa, M.A.N., Paiva, A. & Pacheco, P.M.C.L., 2006, "Tensile-compressive asymmetry influence on the shape memory alloy system dynamics", Chaos, Solitons & Fractals, v.36, n.4, pp.828-842.

7. RESPONSIBILITY NOTICE

The authors are the only responsible for the printed material included in this paper.